Applied Catalysis B: Environmental 129 (2013) 130–136

Contents lists available at SciVerse ScienceDirect

Applied Catalysis B: Environmental

journal homepage: www.elsevier.com/locate/apcatb

Removal of arsenite by coupled electrocatalytic oxidation at polymer–ruthenium oxide nanocomposite and polymer-assisted liquid phase retention

Juan Francisco Rivera[a], Christophe Bucher[a], Eric Saint-Aman[a], Bernabé L. Rivas[b], María del Carmen Aguirre[b], Julio Sanchez[b], Isabelle Pignot-Paintrand[c,1], Jean-Claude Moutet[a,*]

[a] Université Joseph Fourier Grenoble 1, Département de Chimie Moléculaire, UMR CNRS-5250, Institut de Chimie Moléculaire de Grenoble, FR CNRS-2607, BP 53, 38041 Grenoble Cedex 9, France
[b] Faculty of Chemistry, University of Concepción, Casilla 160-C, Concepción, Chile
[c] Centre de Recherches sur les Macromolécules Végétales (CERMAV-CNRS), Institut de Chimie Moléculaire de Grenoble, FR CNRS-2607, Affiliated with Université Joseph Fourier Grenoble 1, BP 53, F-38041 Grenoble Cedex 9, France

ARTICLE INFO

Article history:
Received 27 July 2012
Received in revised form 6 September 2012
Accepted 13 September 2012
Available online 20 September 2012

Keywords:
Ruthenium oxide composites
Electrocatalytic oxidation
Arsenic
Ultrafiltration

ABSTRACT

Nanocomposite materials synthesized by incorporation of ruthenium oxide nanoparticles into a poly(pyrrole-alkylammonium) matrix have been characterized by transmission electron microscopy and by electrochemistry. Ruthenium oxide-based nanocomposites films coated onto carbon appeared efficient electrocatalysts for the oxidation of arsenic(III) into arsenic(V) species at a remarkable low potential, *i.e.* in the 0.3–0.5 V *vs.* Ag/AgCl range. Bulk electrocatalytic oxidation of arsenite solutions could be performed in the presence of a water-soluble poly(quaternary ammonium) salts acting as the supporting electrolyte and also as an As(V) complexing agent, which allowed to combine electrocatalytic oxidation of As(III) with the liquid phase polymer-assisted retention (LPR) technique to efficiently remove arsenic from polluted solutions.

1. Introduction

Arsenic removal is one of the most important areas in water treatment [1]. Arsenic is a highly toxic element creating serious environmental concerns worldwide [2]. The World Health Organization (WHO) provisional guideline value for total arsenic in drinkable water is only 10 ppb and the U.S. Environmental Protection Agency is considering a new standard in the 2–20 ppb range [3,4]. Arsenic is found in both natural surface waters and groundwater, due to the release of arsenic compounds from minerals. In natural waters it occurs in a variety of forms, including soluble, particulate, and organic bound species, but it exists mostly as inorganic pentavalent arsenate (oxidation state +V) and trivalent arsenite (oxidation state +III) species [5]. The latter are more soluble in water and approximately 50 times more toxic than the arsenate ions due to their reaction with enzymes in the human respiratory system [6]. The forms, concentrations and relative proportions of As(V) and As(III) in water vary significantly with changes in the pH and/or the redox properties of natural environments. At high redox potential, arsenic is stabilized as a series of pentavalent (arsenate) oxy-arsenic species: H_3AsO_4, $H_2AsO_4^-$, $HAsO_4^{2-}$, and AsO_4^{3-}, whereas at lower redox potentials, and under most acidic and mildly alkaline conditions, the trivalent arsenic species (arsenite: H_3AsO_3, $H_2AsO_3^-$, $HAsO_3^{2-}$, and AsO_3^{3-}) become stable [7]. The high toxicity and widespread occurrence of arsenic in groundwater have produced a pressing need for new strategies for arsenic removal. Commonly used processes for removing arsenic from water include precipitation–coagulation, lime treatment, adsorption onto metal oxyhydroxydes, ion-exchange, and membrane processes [8–10].

As(III) is more soluble and more mobile than As(V) species. Therefore pre-oxidation of As(III) to As(V) is required to improve the efficiency of the available removal processes. Oxidation of As(III) can be accomplished by using different oxidants and processes, including hydrogen peroxide [11], oxygen and ozone [12], chlorine [13], manganese oxide [14], electrochemical peroxidation [15], iron(III) [16] and titanium dioxide [17] photocatalytic oxidation. In contrast, it is noteworthy that electrochemical oxidation of arsenite into arsenate prior to arsenic removal is limited to a few examples [18–24]. These include mainly electro-coagulation processes in which partial or full electrochemical oxidation of arsenite into arsenate is combined with removal of arsenic by coagulation [19–22].

* Corresponding author. Tel.: +33 476 514 481; fax: +33 476 514 267.
E-mail address: jean-claude.moutet@ujf-grenoble.fr (J.-C. Moutet).
[1] Present address: Minatec, Grenoble Institute of Technology and CNRS 5628, LMGP, Parvis Louis Neel, 38016 Grenoble, France.

0926-3373/$ – see front matter © 2012 Elsevier B.V. All rights reserved.
http://dx.doi.org/10.1016/j.apcatb.2012.09.025

We have recently demonstrated [23–25] that electrochemical oxidation of arsenite combined with membrane ultrafiltration procedures is a promising approach to remove arsenic from contaminated aqueous solutions. Liquid phase polymer-assisted retention (LPR) is well recognized as an efficient technique for the separation of metal ions by ultrafiltration on membranes [26,27], and especially for removing As(V) species from aqueous media [28]. LPR treatment of contaminated aqueous solutions previously submitted to electrocatalytic oxidation of As(III) to As(V) carried out at a bulk platinum electrode [23], and at a platinum–polymer nanocomposite film [24] or iridium oxide-film [25] modified carbon electrodes, has been shown to allow an efficient extraction of hazardous arsenic. The efficiency of this coupled process results from the oxidation of arsenic(III) derivatives into more efficiently extractable arsenic(V) species. Treatment is achieved without adding any chemical oxidants or supporting electrolyte, the cationic water-soluble polymers involved in these processes acting both as As(V) extracting agents and as supporting electrolyte.

Voltammetry is also a straightforward analytic technique allowing the determination of arsenic(III) in solution [29–31]. Electrochemical methodologies thus offer the unique opportunity to simultaneously perform the exhaustive transformation of arsenite to arsenate and to monitor the associated concentration changes.

We now wish to report that the electrocatalytic oxidation of arsenic(III) to arsenic(V) can be efficiently achieved at electrodes modified with a ruthenium oxide-based nanocomposite film. Noble metals and metal oxide nanoparticles dispersed in functionalized and conducting polymer films are promising electrode materials for numerous catalytic and electrocatalytic applications [32–36]. The main reason for employing such composite materials is their excellent electrocatalytic activities which can exceed those of massive materials at relatively low catalyst loads, thus ensuring a more effective use of expensive noble metals or metal oxides. In the present article, we describe the structural and electrochemical characterization of electrosynthesized poly(pyrrole-alkylammonium)–ruthenium oxide nanocomposite films, along with their electrocatalytic properties toward the oxidation of arsenite to arsenate. We also demonstrate the ability of these electrode materials to carry out exhaustive oxidations of arsenite solutions at a remarkable low potential, thereby allowing the combination of electrocatalytic oxidation of As(III) with the LPR technique to efficiently remove arsenic from polluted solutions.

2. Experimental

2.1. Chemicals and reagents

(3-Pyrrol-1-yl propyl)triethylammonium tetrafluoroborate, denoted **PN⁺** (Scheme 1), was prepared according to a previously reported procedure [37]. Potassium ruthenate ($K_2RuO_4{\cdot}H_2O$, Merck), poly(diallyldimethylammonium) chloride (P(ClDDA), Aldrich), sodium(meta)arsenite ($NaAsO_2$, Fluka), acetonitrile (Rathburn HPLC, grade S) and tetra-*n*-butylammonium perchlorate (TBAP, Fluka puriss) were used as received. Distilled water was obtained from an Elgastat water purification system (5 MΩ cm).

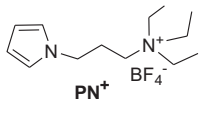

Scheme 1. Pyrrole-containing monomer (**PN⁺**) used in this work.

2.2. Electrodes, electrochemical cells and instrumentation

All electrochemical experiments were performed using a conventional three-electrode system. Electroanalytical experiments were performed using a CHI 660B electrochemical analyzer (CH Instruments). Electrosynthesis of nanocomposites and bulk electrolyses were carried out with an EGG PAR model 273 potentiostat equipped with an *x–y* recorder. Potentials are referred to the Ag|AgCl (3 M KCl) or to the $Ag|Ag^+$ (10 mM in CH_3CN + 0.1 M TBAP) reference electrodes in aqueous and non aqueous electrolytes, respectively. Glassy carbon electrodes (3 mm diameter) were polished with 1-μm diamond paste. All experiments were conducted at room temperature under an argon atmosphere.

2.3. Preparation of the nanocomposite film modified electrodes

The ruthenium oxide-based nanocomposite films were synthesized using a previously reported ion exchange-electroreduction procedure [37,38]. The polymer films (denoted poly**PN⁺**) were grown by potentiostatic oxidative electropolymerization carried out from unstirred solutions of the monomer **PN⁺** (4 mM) in CH_3CN containing TBAP (0.1 M) as supporting electrolyte. The extent of polymerization was controlled through the anodic charge recorded during electrolyses. The amount of pyrrole units in the films and the apparent surface coverage in ammonium units Γ_{N^+} (mol cm^{-2}) were determined, after transfer of the modified electrodes into monomer-free CH_3CN electrolyte, from the integration of the polypyrrole oxidation wave recorded at low scan rate (10 mV s^{-1}), assuming that one in three pyrrole units is oxidized [39].

For the preparation of modified microelectrodes, films of Γ_{N^+} ranging from 2.0×10^{-8} to 6.0×10^{-8} mol cm^{-2} were grown onto glassy carbon disc (3 mm diameter) electrodes by bulk oxidation carried out at E = 0.85 V *vs.* $Ag|Ag^+$ (10^{-2} M) using polymerization charges from 0.5 to 2 mC. In order to obtain clean voltammograms without the large wave for the polypyrrole redox system in the positive potentials region, its electroactivity was destroyed prior to the incorporation of ruthenate anions, by cycling the electrode potential several times between −0.2 and 1.6 V in clean aqueous electrolyte [40]. The resulting C|poly**PN⁺** modified electrodes were then immersed in a 10 mM aqueous solution of $K_2RuO_4{\cdot}H_2O$ for 60 min to ensure a large incorporation of RuO_4^{2-} anions into the polymer film by ion exchange, then they were transferred to a 0.1 M aqueous $LiClO_4$ electrolyte and submitted to bulk reduction at E = +0.2 V *vs.* Ag|AgCl to precipitate ruthenium oxide particles into the polymer matrix. The metal oxide loading in the polymer film was determined from the cathodic charge consumed throughout the reduction process.

Modification of large surface electrodes was achieved by potentiostatic oxidative electropolymerization in acetonitrile electrolyte of **PN⁺** at E = 0.9 V *vs.* $Ag|Ag^+$ (10^{-2} M) onto carbon felt (RVC 2000, 65 mg cm^{-3}, from Le Carbone Lorraine) electrodes (20 mm × 20 mm × 4 mm), using a polymerization charge of 5*C*. This process led to the deposition onto the carbon felt of a polymeric material containing about 10 μmol of ammonium groups (polymerization yield around 45%). Precipitation of ruthenium oxide into the polymer was then performed under the same conditions as described above for the preparation of analytic electrodes, leading to composite films containing about 5.5 μmol of ruthenium oxide.

2.4. Transmission electron microscopy experiments

TEM samples were prepared by precipitation of ruthenium oxide into the polymer deposited onto ITO-coated glass electrodes (1 cm^2) by potentiostatic oxidative electropolymerization in acetonitrile electrolyte of **PN⁺** at 1.1 V *vs.* $Ag|Ag^+$ (10^{-2} M), using charges of 80 mC. The anion exchange-electroreduction process

was then performed four times in order to ensure a larger incorporation of oxide into the polymer film. This led to the formation of a nanocomposite film containing *ca.* 0.16 μmol (29 μg cm^{-2}) of polymer and 0.4 μmol (55 μg cm^{-2}) of ruthenium oxide. Nanocomposite films were peeled off following soaking of the modified ITO electrode in liquid nitrogen, and a piece of film was deposited in a flat mold filled with epoxy resin. The resin was cured at 60 °C for 72 h. Cross-sections through the thickness of the nanocomposites were obtained with a diamond knife at a thickness of 70 nm using a Leica UC6 microtome. The thin sections were collected onto a slotted pattern copper grid (type 75/300) and observed at 300 kV with a JEOL 3010 transmission electron microscope in the laboratory of "Science et Ingénierie des Matériaux et des Procédés" (SIMAP, Grenoble, France). A 50 nm diameter probe was used for energy dispersive X-ray (EDX) analyses; this means that the nanocomposite sampled volumes were of about 55 nm^3.

2.5. LPR procedure

When a solution containing arsenic ions and a water soluble polyelectrolyte such as P(ClDDA) is filtered through a thin membrane, arsenic ions with high binding constant with the soluble polymer are retained whereas uncomplexed ions are permeated through the membrane. The LPR equipment (Amicon) has been previously described [27,28]. The main features are a filtration cell containing a membrane of poly(ether sulfone) with a known exclusion cut-off, connected to a reservoir under pressure.

In this work we used the LPR-washing method, which is an elution method based on continuous diafiltration by addition of solvent at constant volume. Before carrying out the ultrafiltration process, the pH of the electrolyzed solution was adjusted to 8.5. The resulting mixture was stirred for 5 min at room temperature, and then placed in the ultrafiltration cell. The solution was submitted to ultrafiltration and washed with distilled water at the same pH. Ultrafiltration was performed under a total pressure of 3.5 bar using an ultrafiltration membrane of poly(ether sulfone) with a molecular mass cut-off (MMCO) of 10,000 Da. The total cell volume was kept constant during the filtration process. Fractions of 20 mL were collected up to a total volume of 200 mL. All experiments were performed with a solution having a 20:1 polymer:As mole ratio. The total arsenic concentration in the filtrate was measured by graphite furnace atomic absorption spectrometry (GFAAS) using a Perkin Elmer AAnalyst T200 spectrometer. The amount of arsenic species retained within the polymers was calculated as the difference between the measured and the initial concentrations. Results of the arsenic uptake are systematically presented as the percentage of retention *R*(%) *vs*. the filtration factor *Z* (volume of filtrate/volume of the cell). A blank experiment was performed with a solution containing P(ClDDA) and As(III) in a 20:1 mole ratio that had not been previously submitted to electrolysis.

3. Results and discussion

3.1. Electrosynthesis and characterization of poly(pyrrole-alkylammonium)–ruthenium oxide nanocomposites

Electrode surface modification with functionalized polypyrrole films containing cationic [37,41] or complexing [42,43] moieties provides a straightforward and efficient route allowing large amounts of metal ions and complexes to be accumulated onto electrode surfaces. In particular, thin films of alkylammonium-containing polypyrrole [37,41] have been shown to exhibit outstanding potential independent ion-exchange properties that allow extraction and binding of various inorganic salts and complexes, such as iron–sulfur clusters [44], polyoxometallates [45], and metalloporphyrins [46,47]. Furthermore, nanocomposite electrode materials based on noble [24,48] and transition [49] metals have been synthesized by incorporation of anionic metal salts or complexes, followed by their electroreductive precipitation to give zerovalent metal particles.

Preliminary results have shown that poly**PN$^+$** films can be used to trap ruthenium oxide through a two-step procedure involving incorporation of RuO_4^{2-} in the cationic polymer followed by its electroreductive precipitation as ruthenium oxide. However, the structural characterization of the composite electrode materials has not yet been reported and the study of the electrocatalytic activity of this composite electrode material has been limited to the oxidation of benzyl alcohol in an organic electrolyte [37]. In the present work, transmission electron microscopy (TEM) was used to characterize the composite materials (see Section 2 for the preparation of the samples), in particular to gain valuable insights into the size and distribution of ruthenium oxide particles in the polymeric matrix. The TEM analysis (see cross-sectional view depicted in Fig. 1A) of a ruthenium oxide–poly**PN$^+$** film reveals that the thickness of the polymer film is about 0.5 μm. High resolution TEM analyses conducted in both bright field (Fig. 1B) and dark field contrasts (Fig. 1C) also show that the size of the ruthenium oxide particles is in the 2–4 nm range. Furthermore, energy dispersive X-ray (EDX; Fig. 1D) analyses (see Section 2) carried out in the center of the film (Fig. 1A, area (c)), at the substrate/polymer interface (Fig. 1A, area (a)) and at the polymer/electrolyte interface (Fig. 1A, area (b)) have shown that the concentration of ruthenium is similar over the whole structure and that the ruthenium oxide particles are well distributed. All these results clearly demonstrate that this straightforward all-electrochemical procedure leads to the formation of a well defined nanostructured composite material.

The C|poly**PN$^+$**–ruthenium oxide modified electrodes exhibit a well behaved redox response in aqueous electrolytes (Fig. 2A). Considering that the electroactivity of the polymer matrix was purposely destroyed during the fabrication process (see Section 2), the transport of electrons throughout the nanocomposite film only takes place by electron hopping between the metal oxide sites, and the redox waves observed on the cyclic voltammogram are unambiguously attributed to the oxidation of ruthenium oxide species.

According to earlier works on the electrochemical behavior of ruthenium oxide-based anodes [50,51], the peaks observed on the cyclic voltammetry curve recorded in acidic aqueous electrolyte (pH 2.25; Fig. 2A) can be assigned to the $Ru^{IV/III}$ (peak system O_1/R_1; reaction 1 or reaction 2) and $Ru^{VI/IV}$ (peak system O_2/R_2; reaction 3) redox couples.

$$2Ru^{IV}O_2 + H_2O + 2e^- \rightleftarrows Ru_2^{III}O_3 + 2OH^- \quad (1)$$

$$Ru^{IV}O_2 + H_2O + e^- \rightleftarrows Ru^{III}OOH + OH^- \quad (2)$$

$$Ru^{VI}O_4^{2-} + 2H_2O + 2e^- \rightleftarrows Ru^{IV}O_2 + 4OH^- \quad (3)$$

$$Ru^{VII}O_4^- + e^- \rightleftarrows Ru^{VI}O_4^{2-} \quad (4)$$

In addition, the large increase in the anodic current observed over 1 V (O_3) can be attributed to dioxygen evolution [52,53] *via* formation and decomposition of high-valent ruthenium oxides as RuO_4^- (reaction 4; [51]) and RuO_4.

The redox chemistry of ruthenium oxide-based materials in aqueous medium strongly depends on the pH value because the state of ruthenium oxides depends on the formation of surface hydroxyl complexes [51,54]. For instance, the oxidation potential corresponding to the O_1/R_1 redox couple was found to decrease linearly with increasing pH values, from 0.33 V at pH 2 to 0 V at pH 7 (Fig. 2B). The slope of 66 mV/pH unit further confirms that this wave involves removal of one electron/exchanged proton from the ruthenium center (Ru^{IV}/Ru^{III}; reaction 1 or 2). It should also be

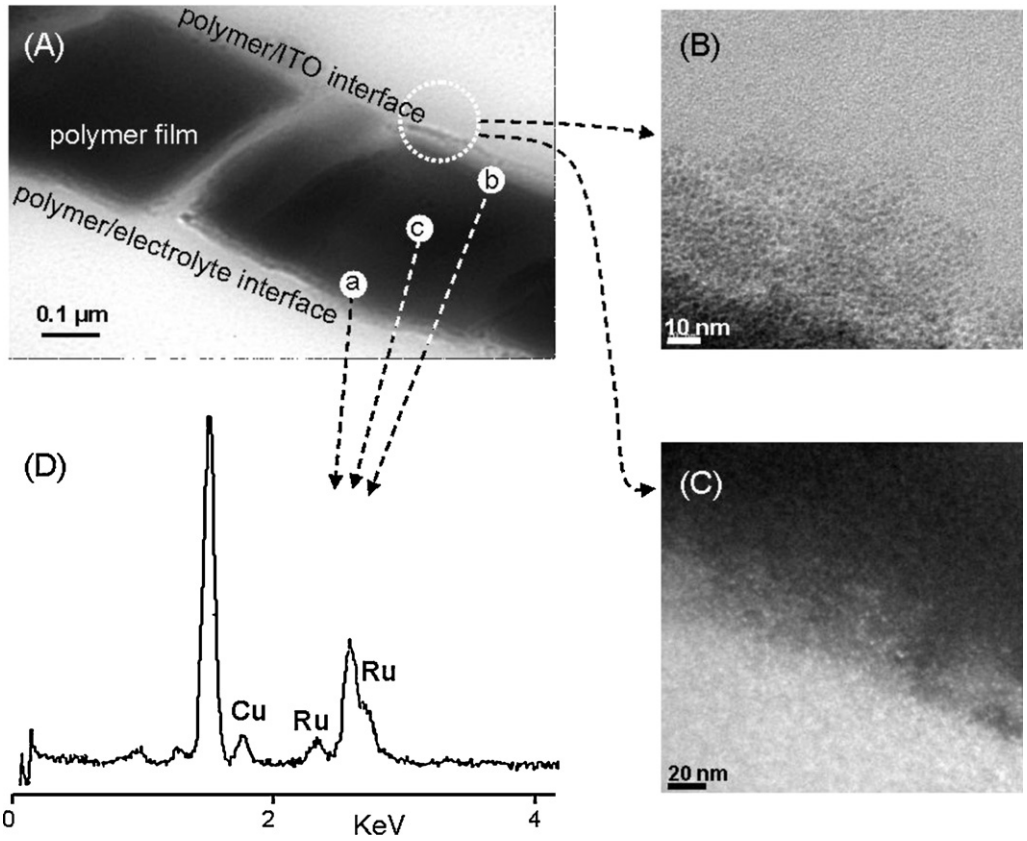

Fig. 1. (A) TEM image of a cross-sectional view of a poly**PN**$^+$ film containing ruthenium oxide; (B) enlargement of (A) under dark field contrast; (C) enlargement of (A) under bright field contrast; (D) EDX analysis performed at different points of the composite film, *i.e.* (a) at the polymer/electrolyte and (b) polymer/ITO interfaces, and (c) in the bulk; Al and Cu signals are due to TEM grid.

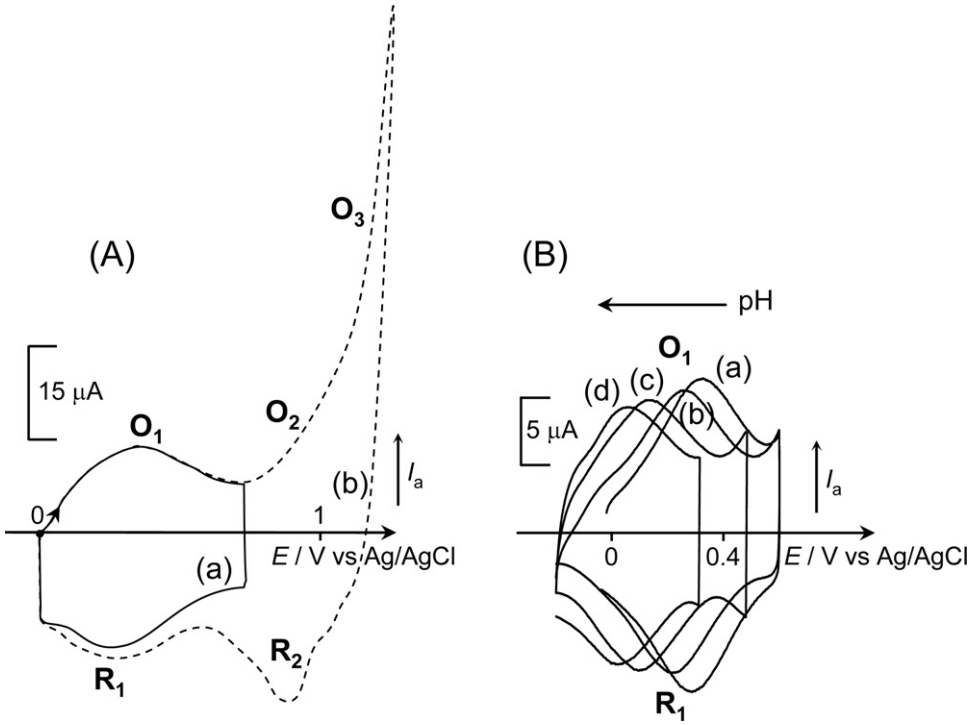

Fig. 2. (A) Cyclic voltammetry curves for a C|poly**PN**$^+$–ruthenium oxide modified electrode recorded in aqueous $Na_2SO_4 + H_2SO_4$ electrolyte (pH 2.25) in the 0–0.6 V (curve (a)) and 0–1.1 V (curve (b)) potential ranges; scan rate 100 mV s^{-1}. (B) Effect of solution pH on the behavior of the first redox peak system (O_1/R_1) of a poly**PN**$^+$–ruthenium oxide film ($\Gamma_{N^+} = 3 \times 10^{-8}$ mol cm^{-2}, $\Gamma_{RuO_2} = 2.6 \times 10^{-8}$ mol cm^{-2}): pH = 2, 3, 5, and 7 for curves (a)–(d), respectively; cyclic voltammetry curves recorded in phosphate buffer, scan rate 10 mV s^{-1}.

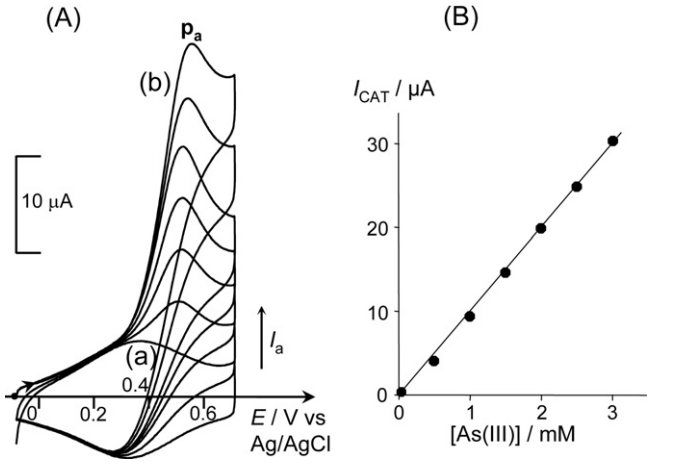

Fig. 3. (A) Cyclic voltammetry curves for a C|poly**PN⁺**–ruthenium oxide electrode (3 mm diameter; $\Gamma_{N^+} = 3 \times 10^{-8}$ mol cm^{-2}, $\Gamma_{RuO_2} = 1.7 \times 10^{-8}$ mol cm^{-2}) recorded in phosphate buffer (pH 2) with increasing amounts of As(III), from 0 (curve (a)) to 3 mM (curve (b)); scan rate 10 mV s^{-1}. (B) Plot of the catalytic current ($I_{CAT} = I_{pa}$ ([As^{III}] ≠ 0) − I_{pa} ([As^{III}] = 0)) *vs.*the concentration of As(III).

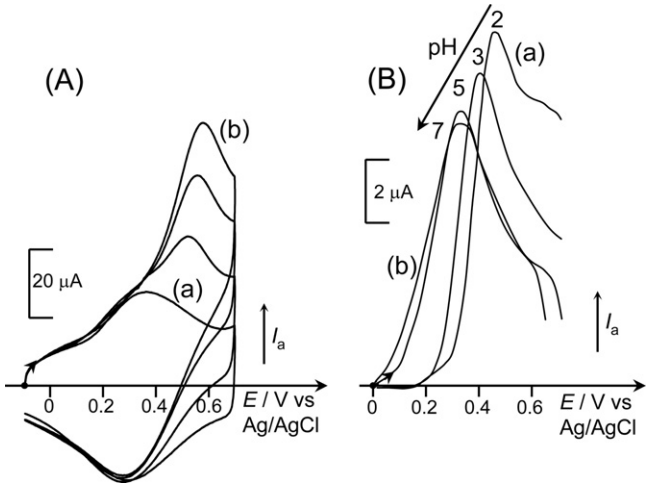

Fig. 4. Cyclic voltammetry curves for a C|poly**PN⁺**–ruthenium oxide modified electrode (3 mm diameter; $\Gamma_{N^+} = 3 \times 10^{-8}$ mol cm^{-2}, $\Gamma_{RuO_2} = 1.7 \times 10^{-8}$ mol cm^{-2}) recorded in phosphate buffer (pH 2) in the presence of increasing amounts of As(III), from 0 (curve (a)) to 3 mM (curve (b)); scan rate 50 mV s^{-1}. (B) Effect of the pH on the catalytic current ($I_{CAT} = I_{pa}$ ([As^{III}] = 1 mM) − I_{pa} ([As^{III}] = 0)) for the oxidation of As(III), from pH 2 (curve (a)) to pH 7 (curve (b)); same other conditions as in (A).

emphasized that the intensity of the O_1/R_1 peak remains the same on going from acidic to neutral pH.

3.2. Electrocatalytic oxidation of As(III) to As(V) at electrodes modified with a poly(pyrrole-alkylammonium)–ruthenium oxide nanocomposite film

The electrocatalytic activity of the electrodes modified with the nanocomposite film toward oxidation of As(III) was first examined by cyclic voltammetry in phosphate buffer (0.1 M, pH 2). We have previously established that oxidation of arsenite is ineffective at a naked glassy carbon electrode and at C|poly**PN⁺**-modified electrodes, with only weak anodic currents observed above 0.9 V [24].

However, a significant catalytic activity toward oxidation of As(III) is brought about by the inclusion of ruthenium oxide particles in poly**PN⁺** films, as revealed by the observation of a large oxidation peak at about 0.5 V. Fig. 3A shows the typical voltammetric response (scan rate 10 mV s^{-1}) recorded at a C|poly**PN⁺**–ruthenium oxide modified electrode upon adding increasing amounts of $NaAsO_2$ to the buffered solution (pH 2). The peak potential gradually shifts toward more positive potential values, from 0.49 V ([As(III)] = 0.5 mM) to 0.54 V ([As(III)] = 3 mM) and the catalytic current I_{CAT}, defined as I_{pa} ([As^{III}] ≠ 0) − I_{pa} ([As^{III}] = 0), increases linearly (r^2 = 0.9979) in the 0.5–3 mM range (Fig. 3B). As expected, I_{CAT} increases as the surface concentration of ruthenium oxide is increased, *i.e.* from 43 μA for $\Gamma_{RuO_2} = 7.8 \times 10^{-9}$ mol cm^{-2} to 50 μA for $\Gamma_{RuO_2} = 1.8 \times 10^{-8}$ mol cm^{-2}, to reach 63 μA for $\Gamma_{RuO_2} = 2.7 \times 10^{-8}$ mol cm^{-2} in the presence of 3 mM As(III), at a scan rate of 50 mV s^{-1}.

As illustrated by the curves in Fig. 3A, the electrocatalytic reaction occurs under these experimental conditions at a higher potential than that of the $Ru^{IV}O_2/Ru_2{}^{III}O_3$ redox couple, *i.e.* in a region where $Ru^{IV}O_2$ is converted into $Ru^{VI}O_4{}^{2-}$, according to Eq. (3). This is clearly observed at a higher scan rate (Fig. 4A). All these data support the assumption that the oxidation of As(III) species is catalyzed by ruthenate ($RuO_4{}^{2-}$) species.

The potential of the catalytic peak progressively decreases with increasing pH, from 0.5 V at pH 2 to 0.3 V at pH 7. It should be noted that the catalytic current I_{CAT} is significantly higher under acidic conditions (pH 2; Fig. 4, curve a) than at neutral pH (Fig. 4, curve b). This electrocatalytic property involving ruthenium oxide particles compares well with those of other nanostructured electrode materials, especially from a potential point of view. For example, the catalytic oxidation of As(III) species in H_2SO_4 electrolyte has been observed in the 0.6–0.85 V range using Pt nanoparticles modified carbon electrodes [31,55], at 0.65 V in a phosphate buffer (pH 4) with iridium-modified boron-doped diamond electrodes [56], at 0.5 V (pH 4.3 [57]) and 0.6 V (pH 3 [25]) on iridium oxide films, and at 0.75 V at a carbon electrode modified with cobalt oxide nanoparticles [58].

3.3. Electrocatalytic oxidation of As(III) to As(V) on the preparative scale

The efficiency of the ruthenium oxide-based nanocomposite material toward the macroscopic oxidation of As(III) to As(V) was checked using modified carbon felt electrodes (see Section 2).

In a typical experiment, the bulk oxidation of an unbuffered aqueous solution (7 mL) containing Na_2SO_4/HNO_3 (0.1 M) and $NaAsO_2$ (3 mM) was conducted in a H-shaped three-compartment cell. The working electrode potential was set at 0.4 V until reaching consumption of the theoretical charge (4 C) required for the two-electron oxidation of arsenic(III) to arsenic(V). The progress of the electrolysis was followed *in situ* from the height of the As(III) oxidation peak recorded at an analytic modified microelectrode. As an example, Fig. 5 shows the progressive decrease in the catalytic current I_{CAT} calculated from cyclic voltammetry experiments recorded at a C|poly**PN⁺**–ruthenium oxide microelectrode during the course of the electrolysis. I_{CAT} reaches almost zero after consumption of a charge of 3.8*C* (Fig. 5, curve d) corresponding to the oxidation of 96% of As(III) into As(V) species. These results confirm that the electrocatalytic oxidation of As(III) is efficiently achieved at ruthenium oxide-modified electrodes, and that full transformation of arsenic(III) to arsenic(V) can be readily performed at a rather low potential and with a high current efficiency.

3.4. Removal of arsenic through the LPR technique combined with full electrocatalytic oxidation of As(III) solutions to As(V)

Previous studies have reported the efficient extraction of As(V) species with water-soluble polymeric complexing agents using the liquid phase polymer-assisted retention (LPR) technique [28]. The retention capacity of As(V) species with the LPR-technique is

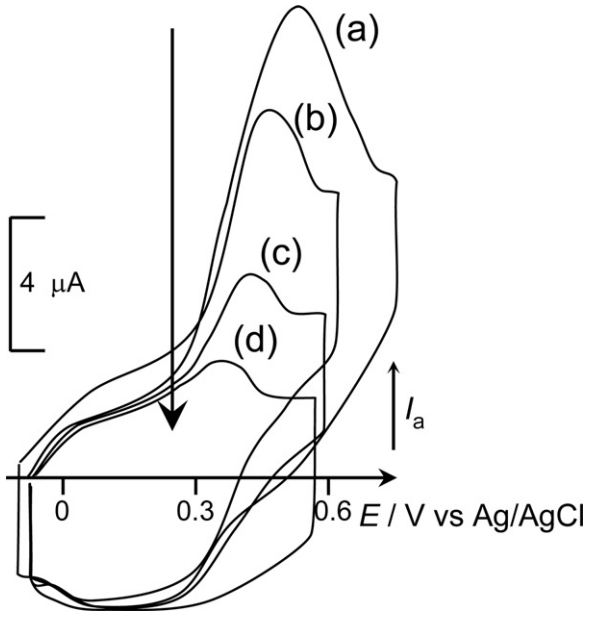

Fig. 5. Cyclic voltammetry curves recorded *in situ* at a C|poly**PN**$^+$–ruthenium oxide modified microelectrode (3 mm diameter) during the course of the electrolysis (E_{app} = 0.4 V) of a 3 mM solution of $NaAsO_2$ at a large surface carbon felt electrode modified with poly**PN**$^+$–ruthenium oxide; curves recorded after charges of (a) 0, (b) 1, (c) 2, and (d) 3.8*C* have been passed; scan rate 10 mV s^{-1}.

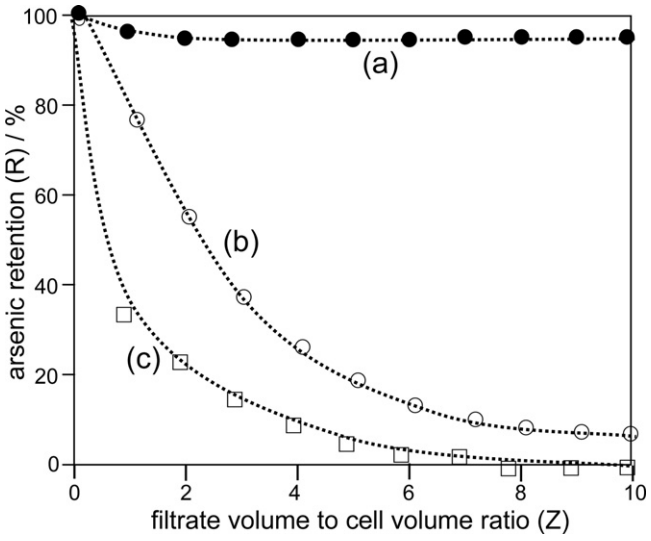

Fig. 6. Arsenic retention profiles obtained after full conversion of As(III) to As(V) by oxidation at 0.5 V at a poly**PN**$^+$–ruthenium oxide carbon felt modified electrode, of a 50 mL solution containing 0.75 mM $NaAsO_2$ and 15 mM P(ClDDA), pH 2.5; filtration experiments were performed on samples of 20 mL, at pH 8.5 (curve (a), ●) and pH 2.5 (curve (b), ○); the blank (curve (c), □) retention profile was obtained at pH = 8.5 using an As(III) solution not submitted to electro-oxidation.

a function of both pH and polymer concentration. The optimum conditions to achieve quantitative removal of As(V) have been established at pH 8 and for a polymer:As(V) molar ratio of 20:1. At this basic pH, where the oxo-dianion $HAsO_4^{2-}$ is the most abundant species, As(V) has been shown to be complexed by polyquaternary ammonium salts and thus efficiently retained in the filtration cell [28].

In the present study aiming at developing arsenic remediation strategies, we have performed preliminary experiments combining electrocatalytic oxidation of arsenic(III) at electrodes modified with ruthenium oxide-based nanocomposite films and the LPR technique. In these experiments, poly(diallyldimethylammonium) chloride (P(ClDDA)) was used simultaneously as the supporting electrolyte and as the extracting agent. In a typical experiment, a solution (50 mL) of arsenite and P(ClDDA), at a polymer:As(III) molar ratio of 20:1 (As(III) 0.75 mM, P(ClDDA) 15 mM) was submitted to electrocatalytic oxidation. The pH of the solution was adjusted to 2.5 with dilute HNO_3, in order to obtain a strong catalytic current. Electrolysis was conducted at E_{app} = 0.5 V, in a one-compartment cell without a separator between the working electrode (poly**PN**$^+$–ruthenium oxide carbon felt modified electrode) and the auxiliary electrode (platinum basket). Under these conditions, the bulk oxidation of As(III) is thus achieved at a much lower potential than those observed using massive platinum electrodes (0.8–0.9 V [23]), a Pt(0)-polymer nanocomposite film modified electrode (0.6–1.1 V [24]), or iridium oxide films (0.8 V [25]).

After consumption of the charge required for the exhaustive oxidation of As(III) to As(V) (≈7.1*C*), 20 mL samples of the resulting electrolyzed solution was submitted to ultra-filtration (see Section 2), and the arsenic concentration in the filtrate was determined by atomic absorption spectrometry. Fig. 6 shows the arsenic (*V*) retention *R vs. Z*, where *Z* is the filtration factor defined as the ratio of the filtrate volume (V_f) to the cell volume (V_o). Arsenic complexation/retention appears inefficient (less than 10%; Fig. 6, curve b) when the LPR experiment is conducted without pH adjustments, *i.e.* at a pH of 2.5 imposed by the experimental procedure. This result is not surprising since arsenate is stabilized as a neutral H_3AsO_4 species and as a monanionic $H_2AsO_4^-$ oxy-arsenic species in acidic media. In contrast, arsenic retention reached more than 96% (see Fig. 6, curve a) when the pH of the electrolyzed solution was adjusted to 8.5 before performing the filtration experiment. Finally, we checked that the recovery of arsenic was 0% at pH 8.5 for a solution containing P(ClDDA) and As(III) in a 20:1 mol ratio that had not been previously submitted to electrolysis (Fig. 6, curve c).

4. Conclusions

The present study demonstrates that ruthenium oxide–polymer nanocomposites are efficient electrocatalysts for the oxidation of arsenite into arsenate at a rather low potential, *i.e.* in the 0.3–0.5 V *vs.* Ag/AgCl range. We have also showed the ability of these nanocomposite electrode materials to carry out bulk electrocatalytic oxidation of arsenite solutions in the presence of a water-soluble poly(quaternary ammonium) salts acting as the supporting electrolyte and also as an As(V) complexing agent, which allowed combined electrocatalytic oxidation of As(III) with liquid phase polymer-assisted retention to remove arsenic from polluted solutions. As compared to our previous work carried out at a bulk platinum electrode, a platinum–polymer nanocomposite film, or at an iridium oxide film modified electrode, the use of a ruthenium oxide-based nanocomposite electrode material allows the bulk electrocatalytic oxidation of arsenic(III) to be performed at a lower potential. It should be emphasized that nanocomposite films can be used simultaneously for the exhaustive transformation of arsenite to arsenate using large surface electrodes, and also to follow the progress of macroscale oxidations of As(III) to As(V) at modified carbon microelectrodes. These experiments thus confirm that the combination of the LPR technique with the electrocatalytic bulk oxidation of arsenic(III) at ruthenium oxide–polymer nanocomposite film modified electrode represents an efficient and promising approach to remediate arsenic in contaminated water.

Acknowledgements

The authors thank ECOS-CONICYT (Grant No. C07E07) and CNRS-CONYCIT (Grant No. 19960), PIA (Grant ACT-130), and CIPA

for financial support. J.F. Rivera thanks the Région Rhône-Alpes for a PhD scholarship.

References

[1] M. Berg, S. Luzi, P.T.K. Trang, P.H. Viet, W. Giger, D. Stuben, Environmental Science and Technology 40 (2006) 5567.
[2] D.K. Nordstrom, Science 296 (2002) 2143.
[3] World Health Organization, http://www.who.int/water_sanitation_health/publications/2011/dwq_guidelines/en/index.html
[4] U.S. Environmental Protection Agency, www.epa.gov/safewater/arsenic.html
[5] V. Lenoble, O. Bouras, V. Deluchat, B. Serpaud, J. Bollinger, Journal of Colloid and Interface Science 255 (2002) 52.
[6] L. Vega, M. Styblo, R. Patterson, W. Cullen, C. Wang, D. Dermolec, Toxicology and Applied Pharmacology 172 (2001) 225.
[7] P.L. Smedley, D.G. Kinniburgh, Applied Geochemistry 172 (2001) 517.
[8] E.O. Kartinen Jr., C.J. Martin, Desalination 103 (1995) 79.
[9] V.K. Gupta, A. Nayak, S. Agarwal, R. Dobhal, D.P. Uniyal, P. Singh, B. Sharma, S. Tyagi, R. Singh, Desalination and Water Treatment 40 (2012) 231.
[10] V.K. Gupta, P.J.M. Carrott, M.M.L. Ribeiro, Suhas, Critical Reviews in Environmental Science and Technology 39 (2009) 783.
[11] A. Voegelin, S.J. Hug, Environmental Science and Technology 37 (2003) 972.
[12] M.-J. Kim, J. Nriagu, Science of the Total Environment 247 (2000) 71.
[13] P. Frank, D. Clifford, US Environ. Prot. Agency Report, EPA-600-52-86r021, 1986.
[14] T.A. Saleh, S. Agarwal, V.K. Gupta, Applied Catalysis B: Environmental 106 (2011) 46.
[15] M. Arienzo, J. Chiarenzelli, R. Scrudato, Fresenius Environment Bulletin 10 (2001) 731.
[16] M.T. Emett, G.H. Khoe, Water Research 35 (2001) 649.
[17] H. Lee, W. Choi, Environmental Science and Technology 36 (2002) 3872.
[18] S. Perez-Sicairos, S.W. Lin-Ho, R.M. Felix, ECS Transactions 3 (2007) 61.
[19] P. Ratna Kumar, S. Chaudhari, K.C. Khilar, S.P. Mahajan, Chemosphere 55 (2004) 1245.
[20] J.A.G. Gomes, P. Daida, M. Kesmez, M. Weir, H. Moreno, J.R. Parga, G. Irwin, H. McWhinney, T. Grady, E. Peterson, D.L. Cocke, Journal of Hazardous Materials 139 (2007) 220.
[21] X. Zhao, B. Zhang, H. Liu, J. Qu, Journal of Hazardous Materials 184 (2010) 472.
[22] I. Alil, V.K. Gupta, T.A. Khan, M. Asim, International Journal of Electrochemical Science 7 (2012) 1898.
[23] B.L. Rivas, M.C. Aguirre, E. Pereira, C. Bucher, G. Royal, D. Limosin, E. Saint-Aman, J.-C. Moutet, Water Research 43 (2009) 515.
[24] J.A. Sánchez, B.L. Rivas, S.A. Pooley, L. Basaez, E. Pereira, I. Pignot-Paintrand, G. Royal, E. Saint-Aman, C. Bucher, J.-C. Moutet, Electrochimica Acta 55 (2010) 4876.
[25] B.L. Rivas, M.C. Aguirre, E. Pereira, C. Bucher, J.-C. Moutet, E. Saint-Aman, G. Royal, Polymers for Advanced Technologies 22 (2011) 414.
[26] B. Ya Spivakov, K. Geckeler, E. Bayer, Nature 315 (1985) 313.
[27] B.L. Rivas, E. Pereira, I. Moreno-Villoslada, Progress in Polymer Science 28 (2003) 173.
[28] B.L. Rivas, M.C. Aguirre, E. Pereira, J.-C. Moutet, E. Saint-Aman, Polymer Engineering and Science 47 (2007) 1256.
[29] D.G. Williams, D.C. Johnson, Analytical Chemistry 64 (1992) 1785.
[30] D.Q. Hung, O. Nekrassova, R.G. Compton, Talanta 64 (2004) 269.
[31] X. Dai, R.G. Compton, Analyst 131 (2006) 516.
[32] A. Malinauskas, Synthetic Metals 107 (1999) 75.
[33] C. Lamy, J.-M. Leger, in: A. Wieckowski, E.R. Savinova, C.G. Vayenas (Eds.), Catalysis and Electrocatalysis at Nanoparticles Surfaces, Marcel Dekker, New York, 2003.
[34] R. Shenar, T.B. Norsten, V.M. Rotello, Advanced Materials 17 (2005) 657.
[35] S. Cattarin, M. Musiani, Electrochimica Acta 52 (2007) 2796.
[36] J.M. Campelo, D. Luna, R. Luque, J.M. Marinas, A.A. Romero, ChemSusChem 2 (2009) 18.
[37] S. Cosnier, A. Deronzier, J.-C. Moutet, J.-F. Roland, Journal of Electroanalytical Chemistry 271 (1989) 69.
[38] S. Cosnier, A. Deronzier, J.-C. Moutet, Inorganic Chemistry 27 (1988) 2390.
[39] A. Deronzier, J.-C. Moutet, Coordination Chemistry Reviews 147 (1996) 339, and references therein.
[40] S. Asavapiriyanont, G.K. Chandler, G.A. Gunawardena, D. Pletcher, Journal of Electroanalytical Chemistry 177 (1984) 229.
[41] L. Coche-Guerente, A. Deronzier, B. Galland, J.-C. Moutet, P. Labbé, G. Reverdy, Y. Chevalier, J. Amhar, Langmuir 10 (1994) 602.
[42] M. Heitzmann, F. Brovelli, L. Basaez, C. Bucher, D. Limosin, E. Pereira, B.L. Rivas, G. Royal, E. Saint-Aman, J.-C. Moutet, Electroanalysis 17 (2005) 1970.
[43] M. Heitzmann, C. Bucher, J.-C. Moutet, E. Pereira, B.L. Rivas, G. Royal, E. Saint-Aman, Electrochimica Acta 52 (2007) 3082.
[44] J.-C. Moutet, C.J. Pickett, Journal of the Chemical Society – Chemical Communications (1989) 188.
[45] B. Keita, D. Bouaziz, L. Nadjo, A. Deronzier, Journal of Electroanalytical Chemistry 279 (1990) 187.
[46] I. De Gregori, M. Carrier, A. Deronzier, J.-C. Moutet, F. Bedioui, J. Devynck, Journal of the Chemical Society – Faraday Transactions 88 (1992) 1567.
[47] F. Bedioui, Y. Bouhier, C. Sorel, J. Devynck, L. Coche-Guerente, A. Deronzier, J.-C. Moutet, Electrochimica Acta 38 (1993) 2485.
[48] I.M.F. de Oliveira, J.-C. Moutet, S. Hamar-Thibault, Journal of Materials Chemistry 2 (1992) 167.
[49] A. Zouaoui, O. Stephan, M. Carrier, J.-C. Moutet, Journal of Electroanalytical Chemistry 474 (1999) 113.
[50] L.D. Burke, J.F. Healy, Journal of Electroanalytical Chemistry 109 (1980) 199.
[51] L.D. Burke, J.F. Healy, Journal of Electroanalytical Chemistry 124 (1981) 327.
[52] R. Kötz, S. Stucki, D. Scherson, D.M. Kolb, Journal of Electroanalytical Chemistry 172 (1984) 211.
[53] M. Wohlfahrt-Mehrens, J. Heitbaum, Journal of Electroanalytical Chemistry 237 (1987) 251.
[54] H. Over, Chemical Reviews 112 (2012) 3356.
[55] S. Sanllorente-Méndez, O. Domínguez-Renedo, M.J. Arcos-Martínez, Electroanalysis 21 (2009) 635.
[56] T.A. Ivandini, R. Sato, Y. Makide, A. Fujishima, Y. Einaga, Analytical Chemistry 78 (2006) 6291.
[57] A. Salimi, M.E. Hyde, C.E. Banks, R.G. Compton, Analyst 129 (2004) 96.
[58] A. Salimi, H. Mamkhezi, R. Hallaj, S. Soltanian, Sensors and Actuators B 129 (2008) 246.